LBL-15175
CONF-820979--2

LBL--15175

DE83 003666

NUCLEAR COLLISIONS FROM AMeV TO ATeV: FROM NUCLEAR TO QUARK MATTER

Miklos Gyulassy

Nuclear Science Division, Lawrence Berkeley Laboratory
University of California, Berkeley, CA 94720

This work was supported by the Director, Office of Energy Research, Division of Nuclear Physics of the Office of High Energy and Nuclear Physics of the U.S. Department of Energy under Contract DE-AC03-76SF00098.

LBL-15175

NUCLEAR COLLISIONS FROM AMeV to ATeV: FROM NUCLEAR TO QUARK MATTER

Miklos GYULASSY

Nuclear Science Division, Lawrence Berkeley Laboratory
University of California, Berkeley, CA 94720

Abstract: The maximum energy density achieved in nuclear collisions is estimated in this energy range. Stopping power and longitudina growth are discussed. We show that for lab energies > 100 AGeV energy ensities high enough to produce a plasma can be reached. Cosmic-ray data support these calculations and suggest a possible novel signature of the plasma phase transition.

As will be stressed repeatedly during this conference, nuclear collisions in the energy range 1 AMeV-1 ATeV (lab kinetic energy per incident nucleon) allow us to explore many novel nonequilibrium and equilibrium aspects of nuclear matter. By colliding "light" nuclei (A < 100), we emphasize nonequilibrium dynamics. With heavy nuclei (A > 100) we hope to probe the bulk equilibrium properties of nuclear matter. Of course, as a function of the incident energy, the relevant degrees of freedom and the dynamical mechanism change several times in this enormous energy range. This is illustrated in fig. 1.

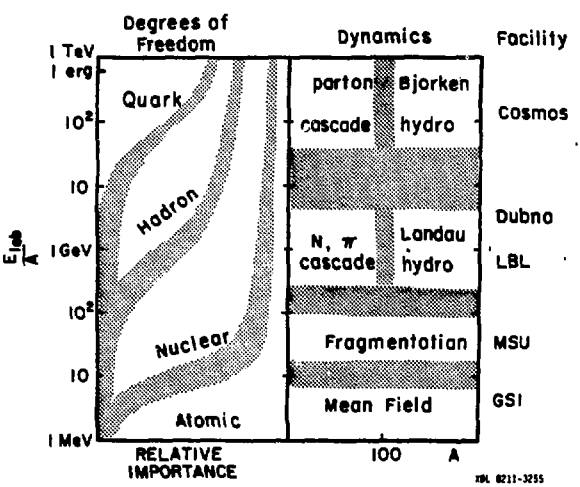

Fig. 1 Overview of central nuclear collisions from MeV to erg per nucleon lab energies. For detailed discussion of the dynamics up to 2GeV see rest of these proceedings. The dynamics above 10 GeV is discussed here and Ref. (9,21).

The relative importance of the various degrees of freedom is illustrated on the left. The dominant dynamical framework for central A + A collisions is illustrated on the right. It is clear that all degrees of freedom from quarks to atomic play some role no matter what the beam energy is. However, at low energies it becomes much more difficult to see the effects of quark degrees of freedom, and at high energies Coulomb effects lead mainly to small final state distortions. A particular degree of freedom becomes most important in a certain energy range. Thus, collective nuclear phenomena are best studied in the 10-400 AMeV domain while quark degrees of freedom are best studied in the few ATeV region.

In this lecture I concentrate on the energy domain $E_{lab} > 10$ AGeV. The question I address is whether ultrarelativistic nuclear collisions can generate high enough energy densities to form a quark-gluon plasma. After reviewing the critical parameters for the deconfinement of hadronic matter, the stopping power of nuclei is estimated. The concept of longitudinal growth and the relation between rapidity density and energy density is discussed. Cosmic-ray data are then analyzed to show that energy densities $\varepsilon >$ 3 GeV/fm^3 could in fact be generated in central $^{238}U + ^{238}U$ collisions in the ATeV range. Finally, a novel signature of the quark-gluon phase transition is suggested.

One of the most striking predictions of Quantum Chromodynamics (QCD) is the deconfinement of hadronic matter at high energy density. This follows from the asymptotic freedom property of QCD. The best estimates for the critical energy density, ε_c, come from Monte Carlo lattice simulations of QCD. The results from two recent calculations[1,2] of the energy density ε versus temperature T in baryon free matter ($\rho_B = 0$) are shown in fig. 2. The dots and triangles are from Ref. (1), where an approximate treatment of quarks is included. The open circles are from Ref. 2 and correspond to pure SU(3) gluon matter. On the left-hand side, the ratio of ε to that of an ideal quark gluon plasma is plotted versus temperature for baryon density $\rho_B = 0$. The energy density of an ideal up-down-glue plasma is given by the Stephan-Boltzmann form[1-3]

$$\varepsilon_{SB}(T,\mu) = \frac{37}{30}\pi^2 T^4 + 3 T^2\mu^2 + \frac{3}{2\pi^2}\mu^4 \qquad (1)$$

where μ is the chemical potential. The baryon density is given by

$$\rho_B = \frac{2}{3\pi^2}\mu^3 + \frac{2}{3} T^2\mu \qquad (2)$$

and the pressure in the plasma is simply

$$P_{SB} = \varepsilon_{SB}/3.$$

In fig. 2, we see that for $T > T_c \sim 200$ MeV, $\varepsilon/\varepsilon_{SB} \approx 1$, and thus QCD predicts that the state of the matter is described well as an ideal plasma. For $T < T_c$ there is a rapid departure from the Stephan-Boltzmann form as confinement sets in.

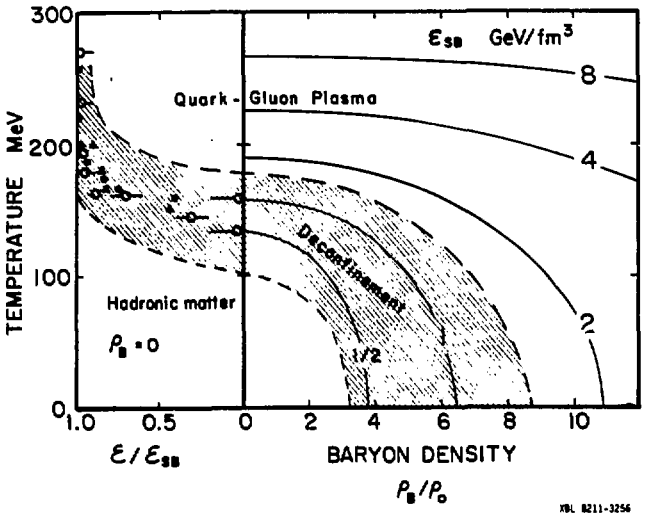

Fig. 2 Phase diagram hadronic matter. Monte Carlo QCD data[1-3] on left indicate existence plasma transition at energy densities ~2GeV/fm^3. Equal ε_{SB} contours, eq. (1), versus T and ρ_B are shown on the right.

The precise nature of the deconfinement transition is still under debate, but it is likely[3]) that for the SU(3) color group the transition is first order. The shaded area around the "data" points is to remind us that systematic uncertainties exist associated with the approximate treatment of quark degrees of freedom and finite lattice size corrections in present calculations and that there is uncertainty in translating the lattice cutoff Λ_L into physical units (MeV).

Based on these and other model calculations at finite baryon density[3]), the following picture of the phase diagram of hadronic matter as a function of T and ρ_B is emerging: Above some critical energy density, ε_C, hadronic matter dissolves into an ideal quark gluon plasma state. A contour plot of the plasma energy density ε_{SB} is shown on the right side of fig. 2. Above the shaded region the actual energy density is very close to ε_{SB}. However, below that region there is a large reduction factor caused by confinement. While the technical definition of the transition temperature[3]) corresponds to $\varepsilon \sim 0.5$ GeV/fm^3, I define the critical temperature, T_C, here as the point where ε reaches ~90% of the Stephan-Boltzmann value. The critical energy density so defined corresponds to $\varepsilon = \varepsilon_{pl} \sim 2$ GeV/fm^3. For $\varepsilon \geq \varepsilon_{pl}$ the matter is essentially in a perturbative plasma phase, while below ε_{pl} there is a complicated mixed hadron-plasma phase.

We now come to the question of whether nuclear collisions can generate energy densities $\varepsilon > \varepsilon_{pl}$. Consider first the stopping power of nuclei as a function incident energy E_{Lab} and atomic weight, A.

In a typical hadron-hadron collision a fraction $\eta \sim 1/2$ of the parallel momentum is lost. In terms of rapidity, y, this momentum loss corresponds to a rapidity shift[4])

$$\Delta y \approx \ln \frac{1}{1-\eta} < 1 \qquad (3)$$

for both hadrons. (Recall that for a particle of mass m and momentum $(p_\parallel, p_\perp)$, $p_\parallel = m_\perp \sinh y$ and $E = m_\perp \cosh y$ in terms of y, and $m_\perp = (m^2 + p_\perp^2)^{1/2}$.)

Therefore, the rapidity of a particle after[5] $\nu \approx 0.65\, A^{0.3}$ <u>independent</u> collisions is

$$y(\nu) = y - \nu\Delta y \quad . \tag{4}$$

We say that a particle is stopped if

$$\bar{\nu} > y/\Delta y \quad . \tag{5}$$

It is important to emphasize that stopping is a frame-dependent concept. If y_L is the lab rapidity ($y_L = 2y_{cm}$), then the particle stops in the nucleon-nucleon cm frame if $y_L < 2\nu\Delta y$. In terms of lab kinetic energy, $E_L = m_N(\mathrm{ch}\, y_L - 1)$, eqs. (3,5) lead then to

$$E_L < \frac{0.5\ \mathrm{GeV}}{(1-\eta)^{2\nu}} \sim 2^{2\nu-1}\mathrm{GeV} \quad . \tag{6}$$

as a necessary condition for a nucleon to stop in the <u>NN center-of-mass (i.e., midrapidity) frame</u>. For ^{238}U, $\nu \approx 3.4$ so most nucleons stop in a central U + U collision in the midrapidity frame if the lab kinetic energy is less than $E_L < 56$ GeV for $\eta = 1/2$. A more refined recent estimate[6] leads to a similar result. Of course eqs. (4-6) cease to hold for energies above which successive collisions are not independent. We shall see explicitely that for $E > 100$ GeV this is indeed the case because of longitudinal growth.

In order to calculate the energy density, we need to estimate the compression ρ_B upon stopping. If the nuclei are thick enough to stop a nucleon in the midrapidity frame (eq. (6)), <u>and</u> the nucleon recoil is instantaneous, then all nucleons will stop in a Lorentz contracted volume $= \gamma_{cm}^{-1}$ x rest frame volume.[6] Therefore, the baryon density is at least [6]

$$\rho_B/\rho_0 = 2\gamma_{cm} \approx \exp(y_L/2) \quad . \tag{7}$$

This leads to an energy density of at least

$$\varepsilon > 2\gamma_{cm}^2 M_N \rho_0 \quad , \tag{8}$$

where $M_N \rho_0 \approx 0.136\ \mathrm{GeV/fm^3}$. To obtain an upper bound on ρ_B consistent with baryon and four momentum conservation, we can use the Rankine-Hugoniot relation. Given an equation of state, $P = \alpha\varepsilon$, the shock compression ρ_{sh} is simply[7]

$$\rho_{sh}/\rho_0 = \alpha^{-1} + (1 + \alpha^{-1})\,\gamma_{cm} \quad . \tag{9}$$

It is important to emphasize that eq. (9) is independent of the shock front thickness only as long as it is smaller than the dimensions of the system. With eq. (9) the energy density is then bounded by

$$\varepsilon < \varepsilon_{sh} = \gamma_{cm} M_N \rho_{sh} \quad . \tag{10}$$

However, ρ_B cannot increase indefinitely with γ_{cm}. There exists a characteristic proper recoil time $\tau_0 \sim (1/2\text{-}1)$ fm/c for the baryon current to change in a collision. In a frame where the nucleon has rapidity y the time required for its baryon number to stop is dilated to τ_0 ch y. Therefore, the minimum stopping distance in the mid rapidity frame is ~

$\gamma_{cm}\,\tau_0$. We can also think of $\gamma_{cm}\,\tau_0$ as the minimum thickness of any shock front in the midrapidity frame. This leads to a bound on the compression

$$\rho_B/\rho_0 \leq g\, R/\tau_0\gamma_{cm} \equiv \rho_B(\tau_0)/\rho_0 \quad , \tag{11}$$

where $g\sim(1\text{-}2)$ is a geometrial factor depending on the detailed spacial distribution of $\rho_B(z)$. We therefore obtain another bound on the energy density

$$\epsilon \leq (gR/\tau_0)\, M_N\, \rho_0 \quad . \tag{12}$$

To illustrate these equations, consider the following (non unique) interpolation formula incorporating the bounds in eqs. (10,12):

$$\epsilon < \gamma_{cm}\, M_N\, [\rho_{sh}^{-2} + \rho_B(\gamma_0)^{-2}]^{-1/2} \quad . \tag{13}$$

This applies only in the energy region $y_L < 5$ where nuclei are thick enough to stop a nucleon in the midrapidity frame. Figure 3 illustrates eq. (13) for several sets of the parameters. The general feature to note is that finite recoil time effects are likely to become important for $E_L > 10$ AGeV and that $\epsilon > \epsilon_{pl}$ may be reached at $E_L \sim$ 10–100 A GeV with nuclear collisions involving >10fm thick nuclei.

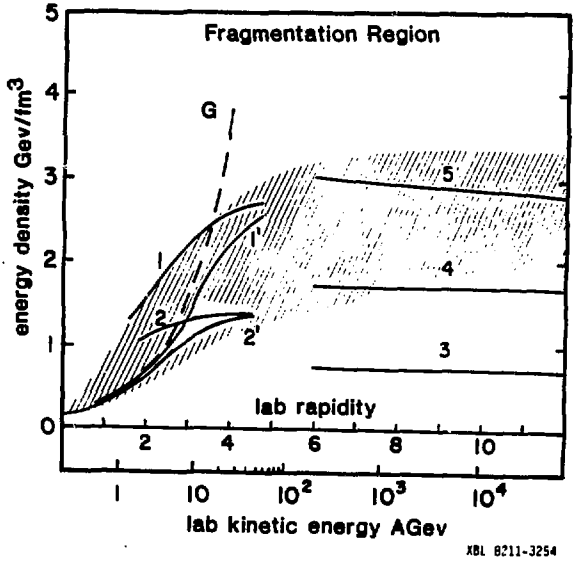

Fig. 3 Energy density achieved in high baryon density regions. Curve G illustrates eq. (8). Shock curves eq. (13) for Stephan-Boltzmann gas ($\alpha = 1/3$), $gR/\tau_0 = 20$, 10 are given by 1 and 2. Stiff equation of a state curves 1', 2' correspond to $\rho_{sh} = 2\gamma_{cm}\,\rho_0$ and $gR/\tau_0 = 20$, 10 resp. in eq. (13). Curves 3,4,5 based on inside-outside cascade[4,9] and eq. (22) with $m_\perp R/2 = 5$, 10, 15 resp. Shaded area is best guess for central U + U collisions.

For lab energies $E_L >$ (10–60) AGeV, uranium is no longer thick enough to stop a nucleon in the NN cm, and nuclear transparency sets in. To estimate

the energy density in this regime we must discuss the concept of longitudinal growth[8,9]. Consider a hadron of mass M suffering a collision in which it is excited to a virtual state of energy $E^{*2} = p_0^2 + M^2$. We want to know how long does it take for this virtual state to decay by emitting a particle of mass m and momentum $(p_\parallel, p_\perp)$. The final state has therefore an energy $E = [(p_0 - p_\parallel)^2 + M_\perp^2]^{1/2} + [p_\parallel^2 + m_\perp^2]^{1/2}$, where $m_\perp^2 = p_\perp^2 + m^2$ and $M_\perp^2 = p_\perp^2 + M^2$. The uncertainty principle states that the amplitude to emit such a particle becomes appreciable only for times[8]

$$t > t(y) \sim \frac{h}{|E^* - E|} \xrightarrow[p_0 >> M]{} 2p_\parallel / m_\perp^2 = \frac{2}{m_\perp} \cosh y \qquad (14)$$

As the rapidity of the emitted particle increases, t increases because of time dilation. We can interpret eq. (14) as follows[9]: in the rest frame of the produce particle it takes $2/m_\perp \sim 1$ fm/c for the particle to come on shell. Before that time it is impossible to disentangle the wavefunction of the final particle from that of the projectile. Since the projectile is assumed highly relativistic (c = 1), the position where the particle is emitted is $z(y) \sim t(y)$. A more detailed estimate of z(y) can be made by invoking the inside-outside cascade (IOC) picture of particle production[9]. In IOC particles follow classical trajectories, $z = t \cdot \tanh y$, but come on shell only at $t = t(y)$. For $t < t(y)$ they propagate as virtual particles with phases interlocked with the projectile. Only for $t > t(y)$ can they participate in incoherent interactions. In this IOC picture the point where a secondary particle comes on shell is thus

$$z(y) = \frac{2}{m_\perp} \sinh y \quad . \qquad (15)$$

Equations (14,15) imply that particles come on shell when their proper time $\tau = (t^2 - z^2)^{1/2}$ reaches $\tau = 2/m_\perp \sim 1$ fm/c, i.e., along a hyperbola in the (t,z) plane. Equations (14,15) specify what is meant by longitudinal growth; at very high energies the interaction region grows very rapidly along the beam direction because of the combined effects of the uncertainty principle and relativistic kinematics.

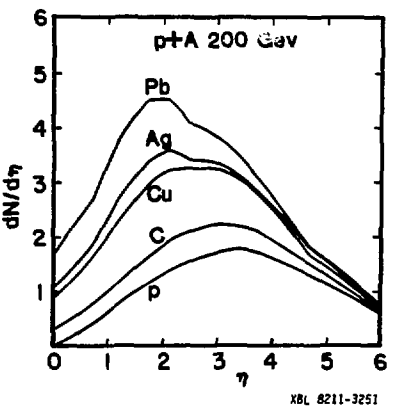

Fig. 4 Pseudo rapidity ($\eta = -\ln \tan \theta_{Lab}/2$) distributions of particles produced in p + A collisions at 200 GeV.[5]

Evidence for longitudinal growth comes from hadron-nucleus data[5,10] as shown in fig. 4.
The striking feature to observe is that for large rapidity secondaries there is virtually no dependence on the target mass, A. This is a direct consequence of longitudinal growth. A pion with rapidity y = 5 can materialize only ~100 fm downstream from the target nucleus! The absence of cascading is particularly evident when the inelasticity $\eta(\nu)$ is computed from the data ($\eta = \int dy\ dN/dy\ E(y)/E_{inc}$). We find that η = 0.5, 0.6, and 0.66 as the target changes from p, Ag, to Pb. This shows that the total energy, radiated into pions increases only very slowly ($d\eta/d\nu \sim 0.07$) with ν, in complete disagreement with the naive independent scattering model, eq. (4). On the other hand, models[10] incorporating nuclear transparency and longitudinal growth have been, on the whole, successful in accounting for high energy hadron-nucleus data. Note finally that the modification of the stopping distance proposed in eqs. (11,12) is consistent with the longitudinal growth of the reaction zone.

Because eq. (15) gives a one-to-one correspondence betwen the rapidity and the production point of a particle, it is possible to compute the energy deposition per unit <u>length</u>, dE/dz, knowing the rapidity distribution dN/dy:

$$\frac{dE}{dz} = m_\perp \cosh y \frac{dN}{dy}\frac{dy}{dz} = \frac{m_\perp^2}{2}\frac{dN}{dy} \quad , \tag{16}$$

where $y = \sinh^{-1}(m_\perp z/2)$. To compute the energy density, ϵ, we must divide dE/dz by the beam area. More precisely, we should take into account the dependence of $\epsilon(z,x_\perp)$ on the transverse coordinate $x_\perp$. If we assume, as in most models, that $\epsilon(z,x_\perp)$ is proportional to the number of struck nucleons along a tube at transverse coordinate $x_\perp$, then for a <u>central</u> (b = 0) nuclear collision

$$\epsilon\ (z,\ x_\perp) \approx \epsilon_{max}\ (1 - x_\perp^2\ /R_{min}^2)^{1/2} \quad , \tag{17}$$

with

$$\epsilon_{max} = \frac{3}{2\pi R_{min}^2}\frac{dE}{dz} \quad . \tag{18}$$

In eqs. (17,18), R_{min} is the radius of the smaller nucleus. Note that $\int d^2x_\perp\ \epsilon = dE/dz$ and that $\langle\epsilon\rangle = 2/3\ \epsilon_{max}$. Inserting $R = 1.18\ A^{1/3}$ and $\langle m_\perp\rangle \sim$ 0.3 GeV, we obtain an estimate for the maximum energy density in the central region

$$\epsilon_{max} \approx 0.1\ \frac{GeV}{fm^3}\ A^{-2/3}\ dN/dy \quad , \tag{19}$$

Clearly, there is at least a factor of 2 uncertainty in the conversion factor in eq. (19). However, eq. (19) allows us to estimate ϵ_{max} from measured rapidity densities.

As a first application of eq. (19) consider pp collisions at ISR energies where $dN/dy \lesssim 3$ for $y_{cm} < 0$. In that case $\epsilon_{max} \lesssim 0.3$ GeV/fm^3, which is too small to create a plasma. Even at $p\bar{p}$ collider energies[11]) $dN/dy \sim 5$ is still too small on the average. The rare events with $dN/dy \sim 10$ lead to 1 GeV/fm^3, but this is still below the Stephan-Boltzmann domain.

Next consider nuclear collisions. At present the only source of experimental information comes from cosmic-ray studies[12,13]). The most spectacular event observed thus far is the so-called JACEE event[12]) Si + Ag at 4-5 ATeV. Over 1000 charged particles were produced with a pseudorapidity distribution shown in fig. 5.

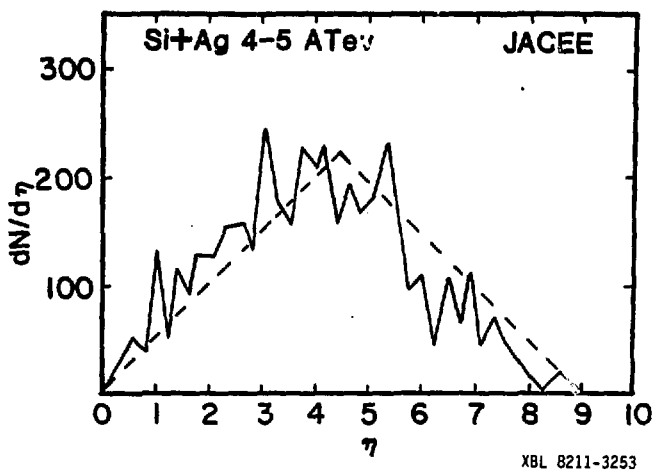

Fig. 5 Pseudo rapidity distribution[12] of Si (4 -5 ATeV) + Ag → 1000 charges + X. The most spectacular nuclear collision ever recorded! Dashed triangle is to guide the eye.

Note that in the central region ($\eta \sim 4$), $dn_{ch}/dy \sim 200$ is observed! This leads, assuming $\langle n_{\pi^0} \rangle = \langle n_{ch} \rangle /3$, to

$$\epsilon_{max}\ (\text{JACEE}) \sim 3\ \text{GeV/fm}^3 \quad . \tag{20}$$

At this point it is important to ask whether this event is just a lucky accident. To answer this question we apply the color neutralization model of ref. 10, which, as was mentioned before, is consistent with hadron nucleus data. For nucleus-nucleus collisions, this predicts

$$\langle n \rangle_{AB} \ / \ \langle n \rangle_{pp} = W_p\ \nu_T\ (1 + \nu_T)^{-1} + W_T\ \nu_p\ (1 + \nu_p)^{-1} \tag{21}$$

where $W_p \approx A_p$ and $W_T \approx A_T\ [1 - (1 - (A_p/A_T)2/3]^{(3/2)}$ are the number of wounded nucleons in the projectile and target for $b = 0$, and ν_p, ν_T are the average number of mean free paths through the projectile and target. Taking[11]) $\langle n_{ch} \rangle \approx 0.88 + 0.44\ \ln s + 0.118\ \ln^2 s \approx 15$ and $W_p = 28$, $W_T = 58$, $\nu_p = 2.4$, $\nu_T = 5.0$ for $b = 0$, eq. (22) predicts $\langle n_{ch} \rangle_{SiAg} \approx 940$, which is close to the observed value. Thus, the JACEE event is not unusual in this respect. Nevertheless, the achieved energy density eq. (20) is well within the Stephan-Boltzmann domain!

A more systematic study of the energy density in the central region is shown in fig. 6. We have included the 15 high energy cosmic-ray events tabulated

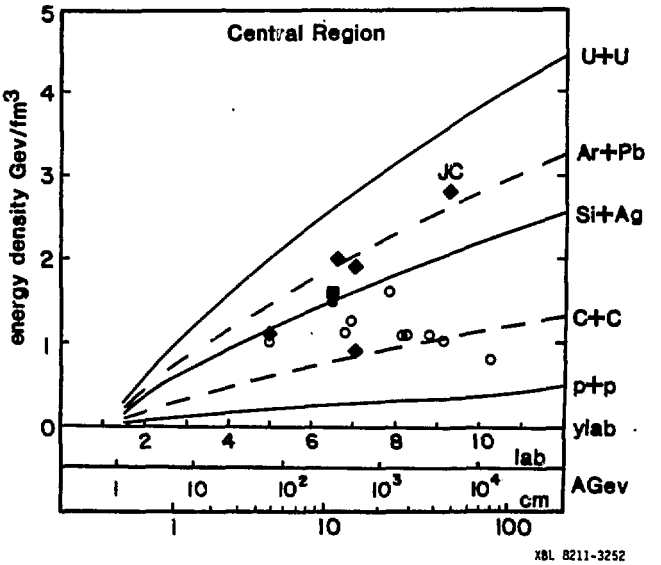

Fig. 6 Maximum energy density achieved in low baryon density regions[14] (midrapidity). Eq. (19) was used to convert measured multiplicities [12,13] into proper energy densities. Diamonds correspond to Si + Ag, square to Ar + Pb, open circles to "light" (α, B, C, N) + Ag collisions. Theoretical estimates for various systems are based on eqs. (19,21) using tube-tube geometry as discussed in text.

in ref. 13. In addition, the theoretical expectations, based on the color neutralization model for a variety of systems are also shown. For these estimates[14]), we have divided the transverse geometry into independent tube-tube collisions and applied eq. (21) to each tube separately. We assumed for simplicity that $dN/dy \approx \langle n \rangle / y_{cm}$ for $y_{cm} = 0$, as appropriate for the rough triangular distributions observed[13]) in nuclear collisions (see also fig. 5). The plotted curves are for the max energy density at $\tau = 1$ and $x_\perp = 0$ for $b = 0$ in the midrapidity frame.

It is remarkable that within the factor of 2 uncertainties in the theoretical curves, the available data are consistent with expectation. We interpret fig. 6 as experimental indication that high enough energy densities can indeed be obtained in nuclear collisions to probe the quark-gluon plasma domain. For Si + Ag the threshold for $\epsilon_{central} > \epsilon_{pl}$ seems to occur ~1 ATeV, while for U + U E_{lab} ~ 100 AGeV seems sufficient.

Now let us return to the fragmentation regions. For $E_{lab} > 100$ AGeV the baryons are certainly not stopped. However, compression caused by recoil and "slow" pion rescattering can lead to high energy densities[9]). An estimate for ϵ_{Frag} can be obtained as follows: only pions with small enough relative rapidity $y_c(A)$ can rescatter within the target or projectile nuclei. Specifically, we must have $z(y) < 2R_A$ for the pion to be produced and interact within the target nucleus. From eq. (15) this means that

$$y_c(A) = \sinh^{-1} m_\perp R_A \lesssim 3 \quad . \tag{22}$$

Therefore, the maximum energy density achieved in the fragmenation regions for $y_{Lab} > 6$ is given approximately by eq. (19) with dN/dy evaluated at $y_{cm} = y_{lab}/2 - y_C(A)$. In fig. 3 results of calculations incuding nuclear recoil energies along the lines of ref. 4 are shown. A triangular rapidity density has been assumed. These results are in accord with earlier results[9]) where $\epsilon_{Frag} \sim 2$ GeV/fm^3 was obtained for U + U. The obvious feature in fig. 3 is that the asymptotic energy densities predicted with the modified stopping scenario (that is valid for $y_{lab} < 5$, eq. (13)) agree within uncertainties with the estimate based on the inside outside cascade model[9]) (that is valid only for $y_{lab} > 6$). Note also that the constancy of ϵ_{Frag} with y_{lab} is expected on grounds of scaling in the fragmentation region. In contrast, the energy density in the central region, fig. 6, continues to grow linearly with y_{Lab} because dN/dy does not scale in this energy range[11]) at $x_F = 0$.

What figs. 3,6 show is that the domain of the quark-gluon plasma is indeed accessible via nuclear collision. They do not show, of course, what experimental signatures could result from such a plasma. Several suggestions have been put forward including strangeness abundancies[15]), dilepton yields[16]), and $\langle p_\perp \rangle$ growth[17]). We suggest a new signature: fluctuations of dN/dy on an event-by-event basis. It has been observed for some time[18]) that for high energy cosmic-ray events with $E_{Lab} > 10$ AGeV there are substantial fluctuations about the mean rapidity density that exceed those expected assuming Poisson statistics. In fig. 5 there is a hint of such fluctuations in rapidity intervals $\Delta y \sim 1$. However, the most spectacular fluctuations are observed in the events discussed in ref. 19. It is also observed that the excess dN/dy fluctuations are correlated with large $p_\perp$ gamma rays (compare fig. 13b and fig. 18 in ref. 19). Could these fluctuations be related to the first order phase transition from the plasma state back into the hadronic world This speculation is fueled by a recent suggestion[20]) that seeds for fluctuations leading to galaxy formation could arise from such a phase transition soon after the Big Bang. If the transition is indeed first order, then the plasma would not simply expand but could burn or detonate as the latent heat is converted into hadronic kinetic energy. Clearly much more thought needs to be given to the dynamics of first order phase transitions. However, it could be that we are already seeing the quark-gluon phase transition in the large fluctuations of dN/dy and the correlation of those fluctuations with high $p_\perp$. A detailed report on these topics is in preparation[14]).

Acknowledgments

Special thanks go to R.E. Gibbs, I. Otterland, H.H. Heckman, and E. Friedlander for introducing me to cosmic-ray data. Helpful discussions with L. McLerran, H. Satz, J. Kapusta, B. Muller, J. Kuti, L. van Hove, J. Rafelski are also gratefully acknowledged. This work was supported by the Director, Office of Energy Research, Division of Nuclear Physics of the Office of High Energy and Nuclear Physics of the U.S. Department of Energy under Contract DE-AC03-76SF00098.

References

1) J. Engels, F. Karsch, H. Satz, Phys. Lett. 113B (1982) 398

2) I. Montvay, E. Pietarinen, PL 110B (1982) 148; 115B (1982) 151

3) See contribution of H. Satz in these proceedings

4) M. Gyulassy, "Formation of Quark-Gluon Plasma in Nuclear Collisions", LBL-14512, to be published in proceedings of Bielefeld conference on quark matter and heavy ion collisions, May 8-16, 1982 (World Scientific Pub. Co., Singapore), eds. M. Jacob, H. Satz

5) J.E. Elias, et al., PR D22 (1980) 13

6) A.S. Goldhaber, Nature 275 (1978) 114; W. Busza, A.S. Goldhaber, Stony Brook preprint ITB-SB-82-22 (1982)

7) H. Stocker, M. Gyulassy, J. Boguta, Phys. Lett. 103B (1981) 269

8) E.L. Feinberg, Phys. Rep. 5 (1972) 237; J. Koplik, A.H. Mueller, PR D12 (1975) 3638; A.S. Goldhaber, PRL 35 (1975) 748

9) R. Anishetty, P. Koehler, L. McLerran, PR 22D (1980) 2793

10) S.J. Brodsky, Proceedings of 1st Workshop on Ultra-Relativistic Nuclear Collisions, Lawrence Berkeley Laboratory, May 1979, LBL-8957, UC-34c, CONF-7905107, p. 419; see also A. Bialas contribution p. 63

11) UA5 Collaboration, PL 107B (1981) 315

12) JACEE Collaboration, in Proceedings of Workshop on Very High Energy Cosmic Ray Interactions, Univ. Penn., April 1982

13) I. Otterlund, E. Stenlund, Physica Scripta 22 (1980) 15

14) M. Gyulassy, L. McLerran, H. Satz, to be published

15) J. Rafelski and B. Muller, PRL 48 (1982) 1066

16) K. Kajantie and H.I. Mietinnen, Z. Phys. C9 (1981) 341

17) L. van Hove, CERN preprint TH.3391 (1982)

18) J. Iwai, N. Suzuki, and Y. Takahashi, Prog. Theor. Phys. 55 (1976) 1537

19) J. Iwai, et al., Nuovo Cim. 69A (1982) 295

20) M. Crawford, D.N. Schramm, Nature 298 (1982) 538

21) J.D. Bjorken, Fermilab preprint Pub-82/44-THY (1982); K. Kajantie and L. McLerran, Univ. Helsinki preprint HU-TFT-82-24 (1982)